



# An Overall Control of BDFIG using Direct Power Control for WECS under Unbalanced Grid Voltage Conditions

A Rahab<sup>1</sup>, H Benalla<sup>1</sup> and F Senani<sup>1</sup>

Département of Electrical Engineering,  
Electrical Engineering Laboratory (LEC)  
Mentouri Brothers University,  
Constantine  
Algeria

---

## ABSTRACT

*The paper presents the complete modelling and control strategy of variable speed wind turbine system (WTS) driven brushless doubly fed induction generators (BDFIG). A back-to-back converter is employed for the power conversion exchanged between BDFIG and grid. The wind turbine is operated on the maximum power point tracking (MPPT) mode its maximum efficiency. The control strategy of CW stator side converter (MSC) combines the technique of MPPT and conventional direct power control. In the control system of the grid side converter (GSC) the direct power control based an improved switching table (IST-DPC) has been used to maintain a constant DC-Link voltage and the reactive power is set to zero. In addition, the behaviours of BDFIG under unbalanced grid voltage conditions are studied and a power compensation scheme is developed to improve the power quality generation. Simulations results using MATLAB/SIMULINK are presented and discussed on a 3.5 KW BDFIG wind generation system based an cascaded doubly fed induction generator demonstrate the effectiveness of the proposed control. several advantages, particularly providing sinusoidal line current when the supply voltage is not ideal.*

**Key Words:** BDFIG, Back-to-back converter, Cascaded doubly fed induction generator, DPC, Imbalanced voltage, Wind power generation.

---

## 1. INTRODUCTION

Wind power has become increasingly popular because of the increasing difficulty of the pollution of the Environment. Enormous efforts have been put in the advancement of WECS, to reduce costs, increase the efficiency and the reliability [1,2], with the sustained and rapid growth of world economy, the energy demand is increasing day by day, but a large amount of fossil fuel is used to lead to the environmental pollution aggravation. The wind energy as a clean and renewable energy accords with the future energy development [3]. The permanent magnet synchronous generator and the doubly fed induction generator based of WECS (PMSG WECS, DFIG-WECS) has become the most popular configuration for wind energy applications on one hand, The DFIG has several advantages including the maximum power capture over a wide speed range and decoupled active and reactive power control. It also

allows the use of a partially rated converter which reduces the system cost [2] [4]. The use of brushes and slip rings associated with the rotors of DFIG decreases the robustness of system and increases the maintenance cost [2],[5-6].

Brushless doubly-fed machines are the evolution of the cascaded induction machine and can be widely used for medium and large wind turbines with limited speed ranges [2–5].

The (BDFIG composed of two stator of different pole numbers called stator of power winding (PW) and stator of control winding (CW) and a special rotor winding. The converters capacity in the CW stator are of almost 25% of the machines rated power, which can operate in a wide speed range including super-synchronous, synchronous and sub-synchronous [4], [7-11], a medium speed machine, enabling the use of a simplified one or two stage gearbox ,excluding the third high-speed stage, known to be the highest failure rate part of the gearbox, hence reducing the weight of the overall drive train and further improving reliability, reduced capital and maintenance costs and has significantly greater LVRT capability[9,10]. The (BDFIG-WECS) retains all the advantages of (DFIG-WECS) and improves reliability by removing brushes and slip rings. Therefore, the (BDFIG-WECS) shows great potential in future wind power generation, especially the large wind turbines and offshore wind farm where maintenance costs are high.[12,13].

Various strategies of control for BDFIG have been used to control of machine side converter (MSC) (the scalar current control, direct torque control, fuzzy power control, sliding mode control, and flux oriented control based on rotor flux or stator flux/voltage orientation [12]. At present, the vector control (VC) is mainly adopted to implement the power decoupling control of BDFIG [7,11,14]. But the (VC) requires the complicated control algorithm and high performance processor, and greatly depends on the BDFIG parameters, which leads to the poor robustness of the system [4]. The direct power control (DPC), derived from direct torque control (DTC), can directly decouple and independently control the active and reactive powers. DPC has a simpler algorithm and less calculation than DTC, and does not need to observe the flux amplitude, which can well solve the problem of the bad real-time of control system caused by the flux observer being sensitive to generator parameter variations. Therefore, DPC of (MSC) has been applied to the (BDFIG) control system in [3-5], [12], the three strategies are based on the same principle with the only difference existing in flux estimation algorithm.

The grid side converter (GSC) control approaches can be classified, as cited in the literature as a vector oriented control (VOC) and direct power control (DPC) [13]. In order to overcome complication in the vector control based on grid voltage or virtual-flux due to the current control loops[14-18], an effective control, namely direct power control (DPC) has been developed [19]. Direct power control (DPC) strategy has become one of the hot research topics in recent Years, because of its fast dynamic response, simple structure, and high power factor, and so on [20, 21]. This strategy is based on a hysteresis control of instantaneous active and reactive powers switching table. Big number of researchers offered different tables of commutation to reduce the complete harmonic distortion (THD) of the currents of line and the losses of commutation [22-26].

This paper is organized as follows: In Section 2, the mathematical model of BDFIG, Wind Turbine and three-phase grid side converter (GSC) is discussed. In Section 3, presents controls of different parts of the (WECS) chain, conventional DPC method is used to control of (MSC), direct power control based improved switching table (IST-DPC) of (GSC) converter to control the voltage of the DC Link is proposed for simplicity, robustness, and excellent performance. Section 4 presents Modified direct power control (MDPC) for MSC under unbalanced grid voltages condition. Section 5 presented some simulation results and discussion finally, the conclusion is provided in section 5.

## 2. MODELING OF WECS COMPONENTS

A typical WECS configuration has been presented in Figure 1

The considered topology consists of: Turbine via a gearbox connected to BDFIG, which the PW stator of BDFIG connected directly to the grid and the CW stator is connected to back-to-back converter, which includes MSC and GSC. The Wind Turbine Aerodynamic Model is given by [27-30]

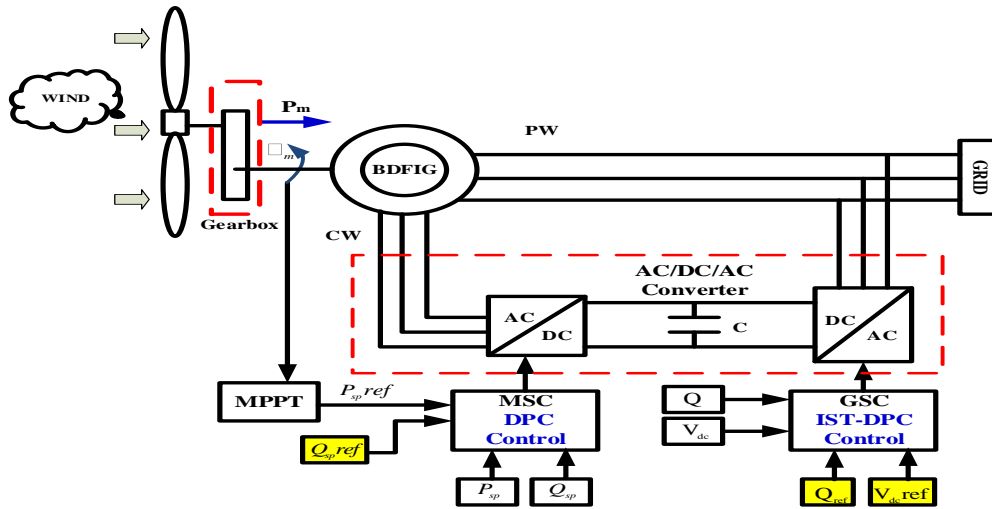


Figure 1: The scheme of variable speed wind turbine system with BDFIG and back-to-back converter system

### 2.1 Mathematical model of BDFIG

The model of the BDFIG in the PW flux frame is expressed as [11].

$$\begin{cases} v_{qsp} = R_{sp} i_{qsp} + \frac{d\psi_{sp}}{dt} + \omega_p \psi_{dsp} \\ v_{dsp} = R_{sp} i_{dsp} + \frac{d\psi_{dsp}}{dt} - (\omega_p - (P_p + P_c) \omega_r) \psi_{qsp} \\ v_{dsc} = R_{sc} i_{dsc} + \frac{d\psi_{dsc}}{dt} - (\omega_p - (P_p + P_c) \omega_r) \psi_{qsc} \\ v_{qsc} = R_{sc} i_{qsc} + \frac{d\psi_{qsc}}{dt} + (\omega_p - (P_p + P_c) \omega_r) \psi_{dsc} \\ 0 = R_r i_{dr} + \frac{d\psi_{dr}}{dt} - (\omega_p - P_p \omega_r) \psi_{qr} \\ 0 = R_r i_{qr} + \frac{d\psi_{qr}}{dt} + (\omega_p - P_p \omega_r) \psi_{dr} \end{cases} \quad (1)$$

$$\begin{cases} \psi_{dsp} = L_{sp} i_{dsp} + M_{spr} i_{dr} \\ \psi_{qsp} = L_{sp} i_{qsp} + M_{spr} i_{qr} \\ \psi_{dsc} = L_{sc} i_{dsc} - M_{scr} i_{dr} \\ \psi_{qsc} = L_{sc} i_{qsc} - L_{scr} i_{qr} \\ \psi_{dr} = L_r i_{dr} + M_{scr} i_{dsc} - L_{spr} i_{dsp} \\ \psi_{qr} = L_r i_{qr} + M_{scr} i_{qsc} - L_{spr} i_{qsp} \end{cases} \quad (2)$$

The aerodynamic torque and instantaneous active, reactive powers of the (PW) are defined as:

$$C_{em} = p_p M_{spr} (i_{qsp} i_{dr} - i_{dsp} i_{qr}) + p_c M_{scr} (i_{dsc} i_{qr} - i_{qsc} i_{dr}) \quad (3)$$

$$P_{sp} = \frac{3}{2} (V_{sdp} I_{sdp} + V_{sqp} I_{sqp}) \quad (4)$$

$$Q_{sp} = \frac{3}{2} (V_{sqp} I_{sdp} - V_{sdp} I_{sqp}) \quad (5)$$

2.2. Model of three-phase PWM converter (GSC & MSC)

The main objective of grid side converter (GSC) is to keep the dc-link voltage constant it is controlled using a VF-DPC based new switching table [23].

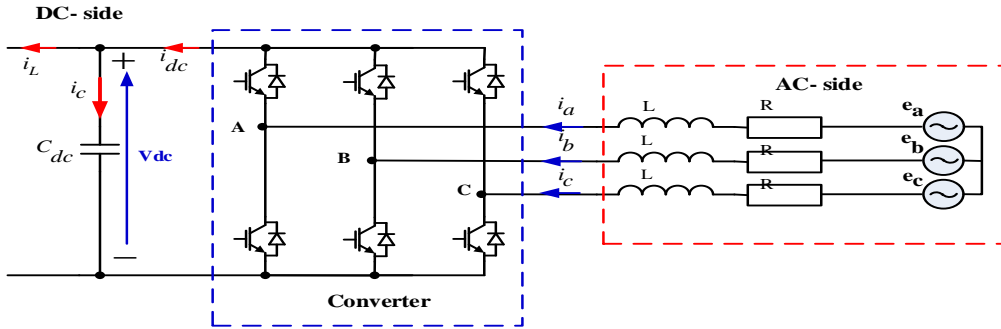


Figure 2 : Block diagram for three-phase PWM rectifier

The mathematical model of converter can be expressed, with following equations [20]:

$$\begin{bmatrix} e_a \\ e_b \\ e_c \end{bmatrix} = R \begin{bmatrix} i_a \\ i_b \\ i_c \end{bmatrix} + L \frac{d}{dt} \begin{bmatrix} i_a \\ i_b \\ i_c \end{bmatrix} + \begin{bmatrix} V_A \\ V_B \\ V_C \end{bmatrix} \tag{6}$$

$$\begin{cases} V_A = \frac{V_{dc}}{3}(2S_a - S_b - S_c) \\ V_B = \frac{V_{dc}}{3}(-S_a + 2S_b - S_c) \\ V_C = \frac{V_{dc}}{3}(-S_a - S_b + 2S_c) \end{cases} \tag{7}$$

$$C_{dc} \frac{dV_{dc}}{dt} = S_a i_a + S_b i_b + S_c i_c - i_L \tag{8}$$

Where: L and R are the inductance and resistance of the chokes, respectively  $e_a, e_b, e_c, i_a, i_b$  and  $i_c$  are the electrical grid voltage and current,  $V_A, V_B, V_C$  are the AC side voltages of the converter.  $S_a, S_b$  and  $S_c$  are the switching states of the rectifier show Figure 5,  $V_{dc}$  is the DC bus voltage.

3.CONTROL STRATEGIES OF WECS

The control strategy used in this paper includes the MPPT algorithm developed in [29], to maximize the power entracte from the Wind, the DPC for MSC by controlling the stator active and reactive powers and the DPC for GSC by controlling the DC-Link voltage and active and reactive powers exchanged with grid.

3.1. Direct power control DPC OF BDFIG with PW stator side converter

The control idea of DPC is derived from DTC. The DPC principle diagram of the BDFIG is shown as Figure.3, which is similar to DTC, the reference active power  $P_{sp}^*$  is set by maximum power tracking strategy according to wind speed. Reference reactive power  $Q_{sp}^*$  is set zero for kept unity power factor, and  $dP, dQ$  are respectively the errors of the active and reactive power. The flux amplitude  $\psi_{sp}$  of the PW stator is approximately constant due to the PW stator is directly connected to the power grid, so the active power  $P_{sp}$  can be controlled by changing the rotational speed and direction of the control winding flux  $\psi_{sc}$ , referring to the DTC method, the reactive power  $Q_{sp}$  can be controlled by changing the flux amplitude  $\psi_{sc}$  of the CW stator [3].

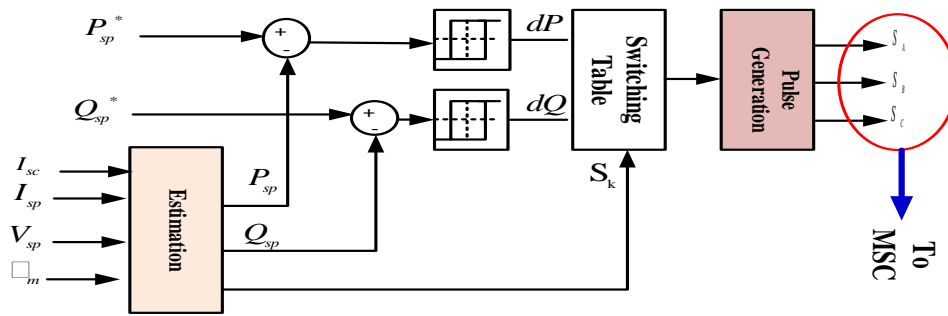


Figure.3: Block diagram of DPC controller for BDFIG

There are eight possible voltage vectors (six active vectors and two null vectors), the  $\alpha$ - $\beta$  plane is divided into six sectors, as shown in Figure 4(b).

The actual output powers  $P_{sp}$  and  $Q_{sp}$  are first estimated, and then compared with the references  $P_{ref}$  and  $Q_{ref}$ . The errors are sent to two fixed band hysteresis comparators to produce digitized signals  $dP$  and  $dQ$ . Finally, the voltage vector is selected from developed in [3],[30], according to  $dP$ ,  $dQ$ , and the position of  $\psi_{sc}$ .

Relationship of CW stator voltage and flux vector is show in Figure4(a) [30].

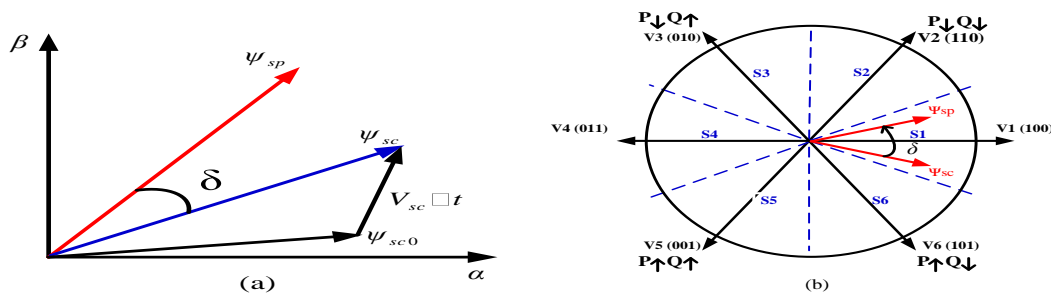


Figure 4 : (a) relationship between voltage vector and flux vector (b) Voltage vectors generated by the inverter and sector division.

In this paper, we have used the same flux estimation principle used in [5]. The PW and CW stator fluxes are estimated in PW stator reference. Then the estimated CW stator flux is transformed to the CW stator reference frame to execute the sector detection algorithm [5].

$$\psi_{sp} = \int (V_{sp} + R_{sp}i_{sp})dt \tag{9}$$

$$\psi_{sc} = R_{sc}i_{sc} - \frac{L_{scm}}{L_{spm}}(\psi_{sp} - L_{sp}i_{sp}) \tag{10}$$

### 3.2 Direct power control of grid side converter

The basic principle of the DPC was proposed by Noguchi [19] and is based on the well know Direct Torque Control (DTC) for induction machines. Figure.5 shows the configuration of the direct instantaneous active and reactive power controller.

The controller control of the active and reactive power with the aid of the use of hysteresis comparators and a improved switching table (IST-DPC) developed in [23] . The new switching schedule improves the quality of line current and results in better dynamic performances as compared with the conventional switching table (ST-DPC) used in [19].

In this configuration, the dc-bus voltage is regulated by Controlling the active power, and the unity power factor operation is achieved by controlling the reactive power to be zero

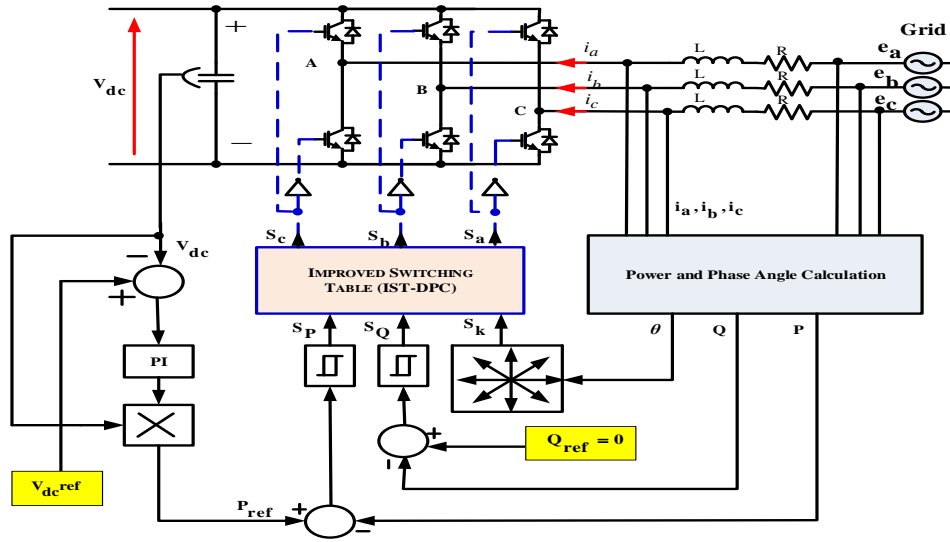


Figure 5 : Block diagram of the conventional DPC

The digitized variables  $S_p, S_q$  and the line voltage vector position  $q = \tan^{-1} \frac{e_a}{e_b} / \frac{\dot{\theta}}{\omega}$  form a digital word, which by accessing the address of lookup table selects the appropriate voltage vector according to the switching table [23]. For this purpose, the stationary coordinates are divided into 12 sectors [19-26]. The instantaneous input active and reactive powers of three phase rectifier are generally defined as:

$$P = e_a i_a + e_b i_b + e_c i_c \quad (11)$$

$$q = \frac{1}{\sqrt{3}} \{ (e_b - e_c) i_a + (e_c - e_a) i_b + (e_a - e_b) i_c \} \quad (12)$$

#### 4. MODIFIED DIRECT POWER CONTROL (MDPC) FOR MSC CONVERTER

When the grid is unbalanced, according to symmetric decomposition theory, an unbalanced three-phase system can be decomposed in three balanced symmetric three phase system, the zero sequence (0), the positive sequence (+), and the negative sequence (-), in this analysis assume a three-wire connection system) [5], as a result, the zero sequences of currents will be zero.

In stationary reference frames, the voltage and current of PW stator are expressed in (13), (14) :

$$V_s = V_{s\alpha} + jV_{s\beta} = (V_{s\alpha}^+ + V_{s\alpha}^-) + j(V_{s\beta}^+ + V_{s\beta}^-) \quad (13)$$

$$I_s = I_{s\alpha} + jI_{s\beta} = (I_{s\alpha}^+ + I_{s\alpha}^-) + j(I_{s\beta}^+ + I_{s\beta}^-) \quad (14)$$

(15) Give the apparent power

$$S = P + jQ = \frac{3}{2} I_{sp}^* V_{sp} \quad (15)$$

After substituting the voltage and current by their values shown in (13) and (14), the active and reactive powers results can be regrouped in three terms:

$$P = \frac{3}{2} \left( (V_{sp\alpha}^+ I_{sp\alpha}^+ + V_{sp\beta}^+ I_{sp\beta}^+ + V_{sp\alpha}^- I_{sp\alpha}^- + V_{sp\beta}^- I_{sp\beta}^-) + (V_{sp\alpha}^+ I_{sp\alpha}^- + V_{sp\beta}^+ I_{sp\beta}^-) + (V_{sp\alpha}^- I_{sp\alpha}^+ + V_{sp\beta}^- I_{sp\beta}^+) \right) \quad (16)$$

$$Q = \frac{3}{2} \left( (V_{sp\beta}^+ I_{sp\alpha}^+ + V_{sp\beta}^- I_{sp\alpha}^- - V_{sp\alpha}^+ I_{sp\beta}^+ - V_{sp\alpha}^- I_{sp\beta}^-) + (V_{sp\beta}^+ I_{sp\alpha}^- - V_{sp\alpha}^+ I_{sp\beta}^-) + (V_{sp\beta}^- I_{sp\alpha}^+ - V_{sp\alpha}^- I_{sp\beta}^+) \right) \quad (17)$$

$$P_2 = V_{sp\alpha}^- I_{sp\alpha}^+ + V_{sp\beta}^- I_{sp\beta}^+ \quad (18)$$

$$Q_2 = V_{sp\beta}^- I_{sp\alpha}^+ - V_{sp\alpha}^- I_{sp\beta}^+ \quad (19)$$

To obtain sinusoidal and balanced line currents; the negative sequence components must be eliminated ( $I_{sp\alpha}^- = I_{sp\beta}^- = 0$ ), and at the (16) and (17) can be written as (20) and (21).

$$P = \frac{3}{2} (V_{sp\alpha}^+ I_{sp\alpha}^+ + V_{sp\beta}^+ I_{sp\beta}^+) + \frac{3}{2} P_2 \tag{20}$$

$$Q = \frac{3}{2} (V_{sp\beta}^+ I_{sp\alpha}^+ - V_{sp\alpha}^+ I_{sp\beta}^+) + \frac{3}{2} Q_2 \tag{21}$$

Under the balanced and perfectly sinusoidal grid voltage supply, there only exists a positive sequence component, and the powers can be described as:

$$P = \frac{3}{2} (V_{sp\alpha}^+ I_{sp\alpha}^+ + V_{sp\beta}^+ I_{sp\beta}^+) \tag{22}$$

$$Q = \frac{3}{2} (V_{sp\beta}^+ I_{sp\alpha}^+ - V_{sp\alpha}^+ I_{sp\beta}^+) \tag{23}$$

It can be seen from (20) and (21) that we want to eliminate the effect of the negative component of the grid; the active and reactive power compensated components can be obtained as:

$$P_{comp} = \frac{3}{2} P_2 \tag{24}$$

$$Q_{comp} = \frac{3}{2} Q_2 \tag{25}$$

The modified DPC strategy is based on the idea of injecting the active power compensated components the original referenced power to achieve control objectives. Figure 6 shows the control diagram.

The new power references that can achieve sinusoidal and symmetric stator current as:

$$P_{ref} = P_{const} + P_{comp} \tag{26}$$

$$Q_{ref} = Q_{const} + Q_{comp} \tag{27}$$

Where  $P_{const}$  and  $Q_{const}$  are the original constant power reference under normal grid conditions.

In this section we illustrate the real-time extraction of positive, negative, sequences from of three phase voltages and current. To achieve that, several methods have been proposed in the literature. The Dual second order generalized integrator (DSOGI-FLL) methods proposed in [31-33] is used to separate the positive and negative sequences (PNSC) of voltage and current. When the proposed method is applied in the DC distribution system. Stable system operation is feasible by performing phase extraction of input voltage, positive sequence voltage extraction only using the SOGI-FLL. Moreover, proposed method reduces the harmonics, which is contained in the input voltage [32,33].

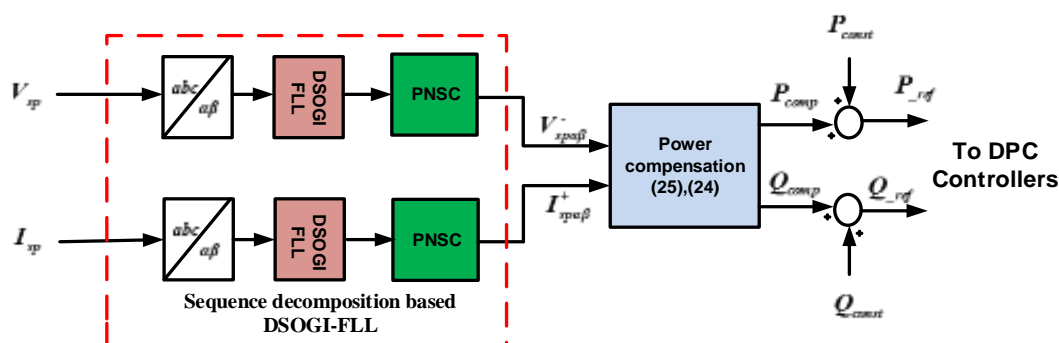


Figure 6 :Control strategy of BDFIG under unbalanced grid voltage conditions. [5].

## 5. SIMULATION RESULTS AND ANALYSIS

In order to verify and the validation of the proposed DPC strategy, the system has been modelled and built in MATLAB/SIMULINK software environment. The dc link voltage is set at 600 V. The (GSC) is controlled using IST-DPC. The (MSC) is exploited to regulate the power flow via BDFIG PW stator to the grid using conventional DPC and MDPC strategy. The BDFIG in simulation based on cascaded doubly fed induction generator .The specific induction generator parameters listed in [34].

The system is analyzed during steady-state and conditions at two case :

- **Case1** : variable speed with balanced grid voltage (wind speed steps from  $V_w=9$  m/s to  $V_w=11$  m/s)
- **Case2** : fixed speed with unbalanced grid voltage (20% supply voltages, wind speed  $V_w=11$  m/s)

### 5.1 Simulation result of case 1:

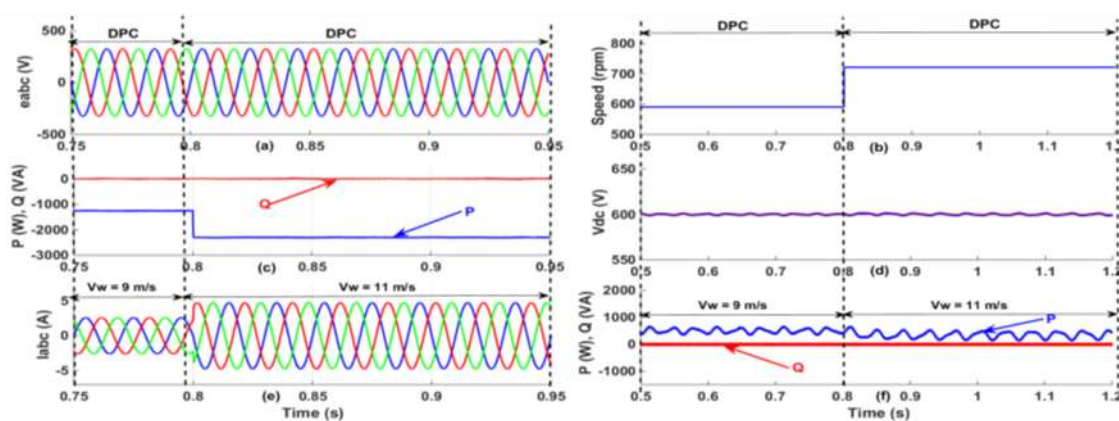


**Figure 7 : Simulation results of (case1). (a) 3- phase voltages waveform of PW stator. (b) generator speed. (c) active power and reactive power of PW stator. (d) DC-link voltage. (e) 3- phase current waveform of PW stator. (f) Active power and reactive power of GSC**

The accurate and smooth of (active and reactive power, DC- link voltage) control in the case1 can be observed from Figure. 8. At  $t=0.8s$ , a wind speed steps from 9 m/s to 11 m/s Figure.7(c) . Figure. 7(f) and Figure. 7(f) (d) shows the excellent dynamic and steady state response of (P), (Q) of GSC and MSC and DC-link voltage. It is important to notice the inherently decoupled control of real and reactive power.

The (PW) stator active power reference is obtained through the MPPT control algorithm, and the GSC power reference is obtained through measured DC-link voltage.

The using improving switching table (IST) in the convensional DPC control scheme notably improved the waveform of the DC-link voltage show Figure 7(d). The control strategy (DPC) of MSC provides balanced and sinusoidal PW stator currents see Figure 7(e).

### 5.1 Simulation result of case 2:

Figure 8 shows the BDFIG behavior using conventional DPC of MSC and (IST-DPC) strategy of GSC under balanced and unbalanced grid voltage. The unbalanced grid voltage is generated at ( $t=0.8$  s) with a 20 % voltage unbalance of phase (a) under fixed wind speed at 11 m/s, Figure 8(a) show the 3 phase voltages waveform of PW stator and Figure 9(b) show the generator speed at fixed wind speed .



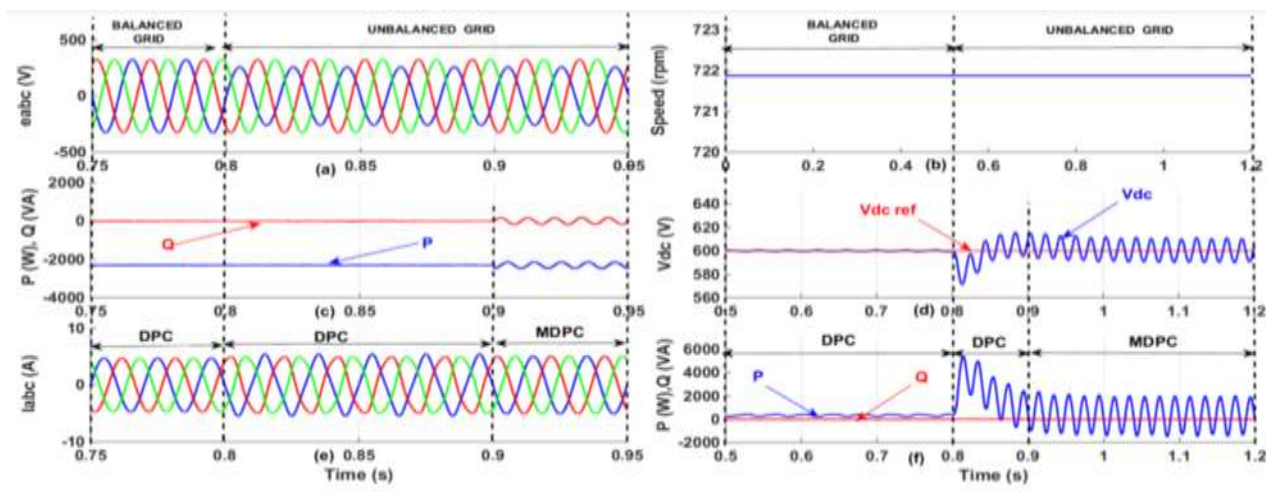


Figure.8: Simulation results of (case2). (a) 3- phase voltages waveform of PW stator. (b) generator speed. (c) active power and reactive power of PW stator. (d) DC-link voltage. (e) 3- phase current waveform of PW stator. (f) Active power and reactive power of GSC

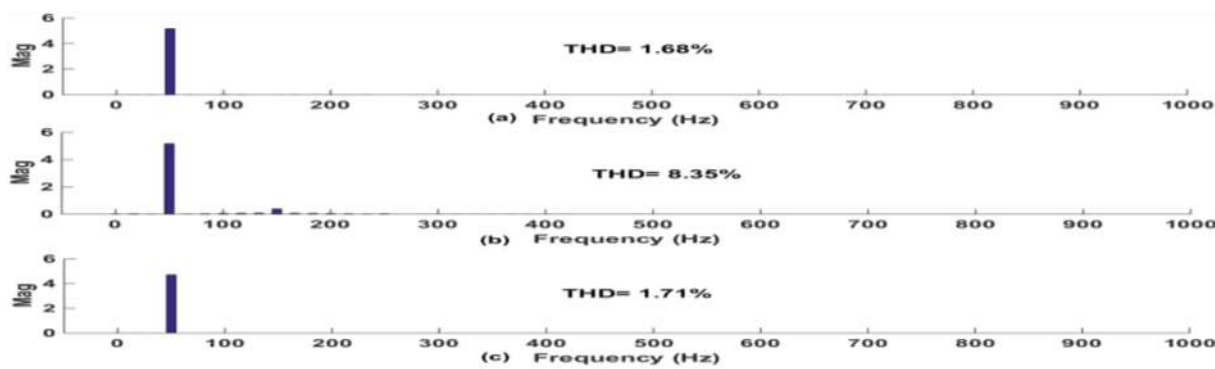


Figure.9 Spectra of PW stator current (a) under balanced grid voltage condition using classical DPC. (b) Under unbalanced grid voltage condition using classical DPC. (c) Under unbalanced grid voltage, condition using MDPC.

At (t=0.8 s to t=0.9 s) It can be seen the active and reactive powers of MSC are smooth and constant due to the excellent control ability of conventional DPC method. However, the active and reactive powers of GSC is oscillated cause unbalanced grid voltages see Figure.8(f). The currents exchanged with the grid (i.e., the PW stator currents) get quite distorted with serious harmonic distortions see Figure.8 (e) and Figure.9 (b), which will pollute the power system. This is unacceptable for grid-connected distributed generations. The waveform of DC-link voltage (Figure.8(d)) clearly indicate that the second-order harmonic component at 100 Hz presented in waveform of DC-link voltage .

At (t=0.9s to t=0.95 s), under unbalanced grid voltage with incorporating the proposed power compensation scheme (MDPC) for MSC, it can be seen that the active and reactive power of PW stator oscillate at twice the grid frequency around their rated values . While the power ripples resulting from an unbalanced part of the supply voltage that it still exists. As well we can see the PW stator currents become sinusoidal and symmetric; thus, power quality is improved significantly.

The presence of an unbalance in voltage supply creates pulsation terms in output DC-link voltage Figure 8(d). As a result, the active powers of GSC oscillate at twice the grid frequency around their rated values. The PW stator current spectra in different scenarios are summarized in Figure. 9. The frequency spectra clearly show that the low-order harmonics can be reduced by employing the modified control strategy (MDPC) under unbalanced voltage supply. The total harmonic distortion (THD) of PW stator current under ideal supply is 1.68% and it is increased to 8.35% under unbalanced supply, and after applying the MDPC strategy the THD is decreased to 1.71%, which meets the IEEE standard 519-1992.

## 6. CONCLUSION

In this paper, a robust direct power control approach applied for wind energy conversion system (WECS) based BDFIG machine has been investigated. The control process is done in a coordinated manner between grid side and generator side. Whereas, conventional DPC has been used for MSC in order to adapt and capture the maximum power available by wind turbine to be fed via PW stator to the grid. GSC control issue focus mainly to ensure constant DC link voltage during system operation. The proposed strategy is verified by simulation for tow cases, which are balanced voltage, unbalanced voltage. It proves its capability of yielding sinusoidal and balanced grid current with unity power factor under unbalanced voltage source. DPC approach of GSC in combination with improved switching table ensures that the dc link voltage is maintained constant (with a little oscillation) and the supply side power factor is kept close to unity under no ideal grid voltage operating conditions. Finally, the proposed IST-DPC and MDPC based BDFIG system obtaining a good power quality on the grid side with a satisfactory power factor and a low THD factor for the PW stator current.

## REFERENCES

- [1] Cheng M, Zhu Y. The state of the art of wind energy conversionsystems and technologies', A review. *Energy Convers Manage.* 2014 ; 88 :332-347.
- [2] Cheng M, Wei X, Han P, Zhu Y, Chen Z. *Modeling and control of a novel dual-stator brushless doubly-fed wind power generation system.* in Proc. Int. Conf. Elect. Mach. Syst. 2014 ;3029-3035.
- [3] Jin S, Shi L, Zhu L, Dong T, Zhang F, Cao W. *Performance comparison of direct power control for brushless doubly-fed wind power generator with different control winding structure.* in Proc. Int. Conf. Elect. Mach. Syst. 2016 ; 3029-3035.
- [4] Shao S, Abdi E, Barati F, McMahan R. Stator-Flux-Oriented Vector Control for Brushless Doubly Fed Induction Generato. *IEEE Transactions on Industrial Electronics.* 2009 ; 56(10), 4220-4228.
- [5] Hu J, Zhu J, Dorrell D G. New Control Method of Cascaded Brushless Doubly Fed Induction Generators Using Direct Power Control. *IEEE Transactions On Energy Conversion.* 2014 ; 29(3) : 771 - 779.
- [6] Sarasola I, Poza J, Rodriguez M A, Abad G. Direct torque control design and experimental evaluation for the brushless doubly fed machine . *Energy Conversion and Management.* 2011 ;52 : 1226-1234,.
- [7] Roberts P.C, McMahan RA, Tavner PJ, Maciejowski JM, Flack TJ. Equivalent circuit for the brushless doubly fed machine (BDFM) including parameter estimation and experimental verification. *IEE Proc. Electr. Power.* 2005.
- [8] Hopfensperger B, Atkinson D J, Lakin R A. Stator flux oriented control of a cascaded doubly-fed induction machine. *IEE Proceedings - Electric Power Applications.* 1999 ;146(6) :597-605.
- [9] Ji K, Zhu J, Gao Y, Zeng C. Vector Control and Synchronization of Brushless Doubly-Fed Machine for High Power Wind Power Generation. 15th International Conference of IEEE on Electrical Machines and Systems (ICEMS). 2012 :21-24.
- [10] Wei X, Cheng M, Han P, Wang W, Luo R. *Comparison of control strategies for a novel dual-stator brushless doubly-fed induction generator in wind energy applications.* 18<sup>th</sup> International Conference on Electrical Machines and Systems (ICEMS). 2015 :1039-1045.
- [11] Wei X, Cheng M, Wang Q. *Direct power control strategies of cascaded brushless doubly fed induction generators.* 42<sup>nd</sup> Annual Conference of the IEEE IECON. 2016 : 23-26.
- [12] Poza J, Oyarbide E, Sarasola I, Rodriguez M. Vector control design and experimental evaluation for the brushless doubly fed machine. *IET Electr. Power Appl.* 2009; 3(4): 247-256.
- [13] Allagui M, Hasnaoui O. A 2 MW direct drive wind turbine vector control and direct torque control techniques comparison. *J. energy South. Afr.* 2014; 25(2): 117-126.
- [14] Prasad A, Ziogas P, Manias S. An active power factor correction technique for three-phase diode rectifiers. *IEEE Trans. Power Electron.* 1991 ;6(1) :83–92.
- [15] Kazmierkowski M. P, Malesani L. Current control techniques for three-phase voltage-source PWM converters: A survey. *IEEE Trans. Ind. Electron.* 1998 ;45(5) :691 –703.
- [16] Pedro V, Marques G. D. DC voltage control and stability analysis of PWM-voltage-type reversible rectifier. *IEEE Trans. Ind. Electron.* 1998 ;45(2) :263–273.
- [17] Nor Azizah Yusoff, Azziddin M. Razali, Kasrul Abdul Karim, Tole Sutikno, Auzani Jidin. A Concept of Virtual-Flux Direct Power Control of Three-Phase AC-DC Converter. *International Journal of Power Electronics and Drive System (IJPEDS).* 2017; 8(4): 1776- 1784.
- [18] Mohseni M, Islam S, Masoum M A S. Enhanced hysteresis-based current regulators in vector control of DFIG wind turbines. *IEEE Trans. Power Electron.* 2011 ;26(1) :223–234.
- [19] Noguchi T, Tomiki H, Kondo S, Takahashi I. Direct power onrol of PWM converter without power-source voltage sensors. *IEEE Transactions on Industry Applications.* 1998 ;34(3) :473– 479.
- [20] Malinowski M , Kazmierkowski M. Simple Direct Power Control of Three-Phase PWM Rectifier Using Space Vector Modulation? A Comparative Study. *EPE Journal.* 2015 :27-34.
- [21] Li Xiang, Han Minxiao. Direct Virtual Power Control. *TELKOMNIKA Indonesian Journal of Electrical Engineering.* 2014; 12(7): 5144- 5153.
- [22] Bouafia A, Gaubert JP, Krim F. *Analysis and design of new switching table for Direct Power Control of three-phase PWM rectifier.* Proceedings of IEEE 13<sup>th</sup> Power Electronics and Motion Control Conference, EPE-PEMC. 2008.

- [23] Baktash A, Vahedi A, Masoum M. *Improved switching table for Direct Power Control of three-phase PWM rectifier*. Proceedings of Australasian Universities Power Engineering Conference, AUPEC; 2007 :1–5.
- [24] Eloy-Garcia J, Alves R. *DSP-based Direct Power Control of a VSC with voltage angle estimation*. IEEE/PES Transmission and Distribution Conference and Exposition, TDC'06;Latin America. 2006 :1–5.
- [25] Razali A M , Rahman M A, George G, Rahim N A. Analysis and Design of New Switching Lookup Table for Virtual Flux Direct Power Control of Grid-Connected Three-Phase PWMAC–DC Converter''. *IEEE Transactions on Industry Applications*. 2015 ; 51(2) : 1189 - 1200.
- [26] Norniella J G, Cano J M, Orcajo G A, Rojas C H, Pedrayes J F, Cabanas M F, Melero M G. Improving the Dynamics of Virtual-Flux-Based Control of Three-Phase Active Rectifiers. *IEEE Transactions on Industry Applications*. 2015 ;51(2).
- [27] Heier S. *Grid Integration of Wind Energy Conversion Systems*. John Wiley & Sons Ltd, ISBN 0-471-97143-X, 1998.
- [28] Rahab A, Senani F, Benalla H. Direct Power Control of Brushless Doubly-Fed Induction Generator Used in Wind Energy Conversion System. *International Journal of Power Electronics and Drive System (IJPEDS)*. 2017 ;8(1):417-433.
- [29] Jin S, Zhang F G, Li Y X. *robust control for VSCF brushless doubly-fed wind power generator system*. In: Proceeding of the IEEE international Conference on Automation and Logistics, Shenyang, China. 2009 :71–475.
- [30] Bing li , shi liu, 'study on direct torque control strategy of brushless doubly-fed induction generator for wind power generation', In: journal of computational system december 15,2014.
- [31] Moźdzynski K, Rafał K, Bobrowska-Rafał M. Application of the second order generalized integrator in digital control systems. *In: Archives Of Electrical Engineering*. 2014 ;63(3) :423-437.
- [32] Rodriguez P, Luna A, Ciobotaru M, Teodorescu R, Blaabjerg F. *Advanced Grid Synchronization System for Power Converters under Unbalanced and Distorted Operating Conditions*. in Proc. IEEE Ind. Electron. Conf. (IECON'06). 2006 : 5173-5178.
- [33] Rodriguez P, Luna A, Etxeberria I, Hermoso, J R, Teodorescu R . *Multiple second order generalized integrators for harmonic synchronization of power converters*. Energy Conversion Congress and Exposition, 2009. ECCE 2009. IEEE , 20-24 Sept. 2009 : 2239- 2246
- [34] Amar Bentounsi, Hind Djeghloud, Hocine Benalla, Tahar Birem, and Hamza Amiar. Computer-Aided Teaching Using MATLAB/Simulink for Enhancing an IM Course With Laboratory Tests. *IEEE Transactions on Industrial Electronics*. 2011; 54(3):479-491.